

## Synthesis of Macroporous Polymer Beads by Suspension Polymerization Using Supercritical Carbon Dioxide as a Pressure-Adjustable Porogen

Colin D. Wood and Andrew I. Cooper\*

Donnan and Robert Robinson Laboratories,  
Department of Chemistry, University of Liverpool,  
Crown Street, Liverpool L69 7ZD, U.K.

Received August 30, 2000

Revised Manuscript Received November 6, 2000

This paper describes the preparation of macroporous polymer beads by oil-in-water (O/W) suspension polymerization using supercritical carbon dioxide (scCO<sub>2</sub>) as the porogenic solvent. Carbon dioxide is an inexpensive, nontoxic, and nonflammable solvent alternative for polymer synthesis and processing.<sup>1</sup> Unlike liquids, supercritical fluids (SCFs) are highly compressible, and the solvent properties can be varied over a wide range by changing the density. In principle, this allows control over variables such as phase behavior, and should permit “tuning” of certain chemical reactions and polymerizations.<sup>2</sup> DeSimone and others have shown that scCO<sub>2</sub> is a versatile medium for both homogeneous and heterogeneous polymerization.<sup>3</sup> Previously, we synthesized cross-linked divinylbenzene-based polymers in scCO<sub>2</sub> by free-radical precipitation polymerization and dispersion polymerization.<sup>4</sup> Microparticulate powders (0.4–10 μm) were formed, but in all cases, the polymers were found to be completely nonporous. More recently, we showed that these reaction conditions can be modified to generate well-defined macroporous polymer monoliths, thereby using scCO<sub>2</sub> as a porogenic solvent.<sup>5</sup> We show here that this technique can be extended to the synthesis of macroporous polymer beads and that the porosity in the beads can be controlled by varying the CO<sub>2</sub> density.

Macroporous polymers are important in a wide range of applications such as ion-exchange resins, chromatographic separation media, solid-supported reagents, and supports for combinatorial synthesis.<sup>6,7</sup> Unlike gel-type polymers which swell in the presence of an appropriate solvent, the cross-link density in macroporous polymers is sufficient to form a permanent porous structure which persists in the dry state. Macroporous polymers are usually synthesized as beads (typical diameter = 10–1000 μm) by O/W suspension polymerization<sup>8</sup> in the presence of a suitable porogen. The porogen may be an organic solvent which is miscible with the monomers<sup>9</sup> or, less commonly, a linear polymer which is soluble in the monomer phase.<sup>10</sup> In general, porogens that are “good” solvents for the growing polymer network tend to give rise to smaller pores and higher surface areas than porogens that are “bad” solvents.<sup>9</sup> This is because the degree of solvation imparted by the porogen affects the phase separation process which occurs during polymerization, thus determining the physical structure of the porous channels.<sup>7</sup> Control over average pore size, pore size distribution, and surface area can be achieved by optimization of reaction variables such as the nature and proportion of the porogen,<sup>9,10</sup> the percentage of cross-linker in the monomer mixture,<sup>11</sup> and the structure of the cross-linker<sup>12</sup> and also by the use of chain

Table 1. Suspension Polymerization of TRIM Using ScCO<sub>2</sub> as the Porogen<sup>h</sup>

	pressure (bar)	stirring speed (rpm)	mean particle diam (μm) <sup>a</sup>	intrusion vol (cm <sup>3</sup> /g) <sup>b</sup>	median pore diam (nm) <sup>b</sup>	surface area (m <sup>2</sup> /g) <sup>c</sup>	yield (%)
1	1	600	180 (44)	0.00	<i>d</i>	<5	68
2	100	600	80 (36)	0.28	(19) <sup>e</sup>	<5	41
3	200	600	110 (33)	1.05	2206	222	70
4	300	600	128 (25)	1.23	110	253	92
5	400	600	114 (40)	0.69	40	478	90
6	300	300	412 (13)	0.42	(84) <sup>e</sup>	<5	70
7	300	1800	46 (11) <sup>f</sup>	1.13	735	366	44
8 <sup>g</sup>	300	600	87 (38)	0.93	102	37	64

<sup>a</sup> Mean diameter calculated from >100 particles. Figure in parentheses = percentage coefficient of variation, CV, where  $CV = (\sigma/D_n) \times 100$ .  $\sigma$  = standard deviation in particle diameter (μm).  $D_n$  = mean particle diameter (μm). <sup>b</sup> Measured by mercury intrusion porosimetry over the pore size range 7 nm–20 μm. <sup>c</sup> Calculated from N<sub>2</sub> adsorption/desorption isotherms by applying the Brunauer–Emmett–Teller method. <sup>d</sup> Nonporous sample. <sup>e</sup> Sample has a relatively low pore volume and exhibits a broad, flat pore size distribution. Thus, the median pore diameter does not provide much useful information in this case. <sup>f</sup> CV value is calculated for whole beads. A significant proportion of fractured beads and “fines” was also observed. <sup>g</sup> Monomer mixture = TRIM (20% v/v) + MMA (80% v/v). <sup>h</sup> Reaction conditions: 20% w/v trimethylolpropane trimethacrylate (TRIM), 2,2'-azobis(isobutyronitrile) (AIBN), 2% w/v, poly(vinyl alcohol) (0.5% w/v based on volume of H<sub>2</sub>O,  $M_w$  = 88 000 g/mol, 88% hydrolyzed), 60 °C, 6 h.

transfer agents.<sup>13</sup> However, to achieve *fine* control over porosity is not always straightforward. For one thing, the porous structure which develops can be remarkably sensitive to small changes in polarity of the porogenic solvent or solvent mixture. This has also been noted in the synthesis of continuous macroporous polymer monoliths.<sup>14</sup> Thus, the development of alternative methods for controlling porosity in macroporous polymers may offer distinct advantages.

In this study, we have exploited the fact that the solvent strength of scCO<sub>2</sub> can be tuned continuously over a significant range by varying the density.<sup>1,2</sup> As such, scCO<sub>2</sub> can be thought of as a “pressure-adjustable” porogen. In a typical reaction, a mixture of monomer [trimethylolpropane trimethacrylate (TRIM)], initiator [2,2'-azobis(isobutyronitrile) (AIBN)], and scCO<sub>2</sub> was suspended in water with stirring in the presence of a stabilizer [0.5% w/v poly(vinyl alcohol)] to inhibit droplet coalescence.<sup>15</sup> All polymerizations were carried out in a stainless steel high-pressure vessel fitted with an impeller stirrer (manufactured by New Ways of Analytics). Tandem reactions were carried out in a high-pressure view cell equipped with a sapphire window for observation of phase behavior.<sup>4,5</sup> This allowed us to ascertain the degree of miscibility of the monomer phase with CO<sub>2</sub>. Table 1 summarizes the results of a series of polymerizations carried out under various conditions. In the absence of CO<sub>2</sub>, the O/W suspension polymerization of TRIM led to polymer beads with an average diameter of 180 μm (entry 1). Analysis by scanning electron microscopy (SEM), mercury intrusion porosimetry, and N<sub>2</sub> adsorption/desorption showed that the beads were nonporous, as reflected by the low surface area (<5 m<sup>2</sup>/g). The reaction was repeated in the presence of scCO<sub>2</sub> over a range of pressures while keeping all other variables constant (entries 2–5).

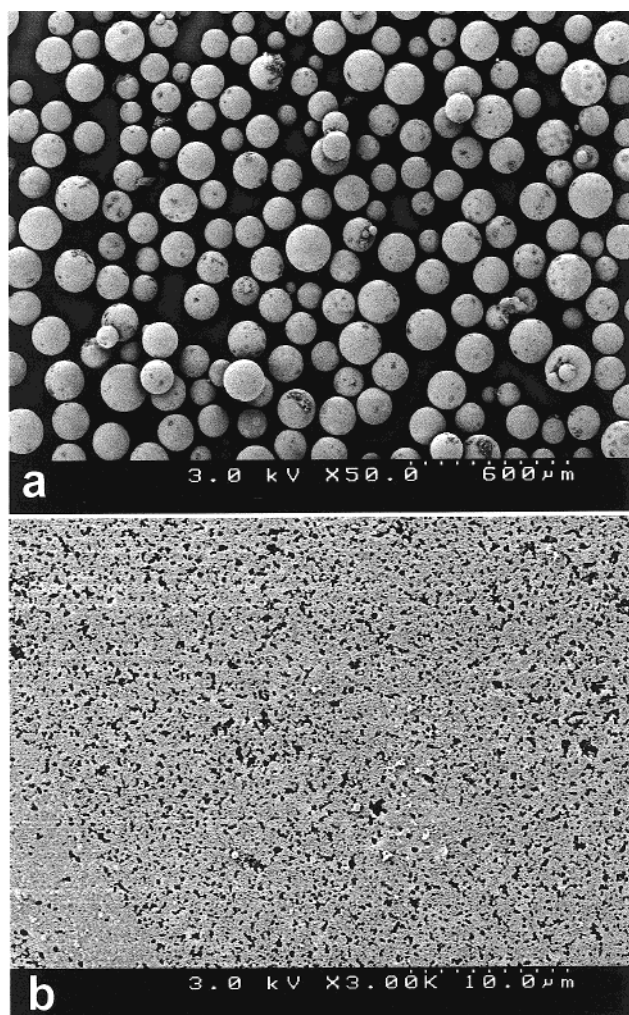


**Figure 1.** Electron micrographs of macroporous polymer beads synthesized using  $\text{scCO}_2$  as the porogen (300 bar). Average bead diameter =  $128 \mu\text{m}$ . (a) Scale bar =  $600 \mu\text{m}$ . (b) Magnification of bead surface showing porous structure, scale bar =  $10 \mu\text{m}$ .

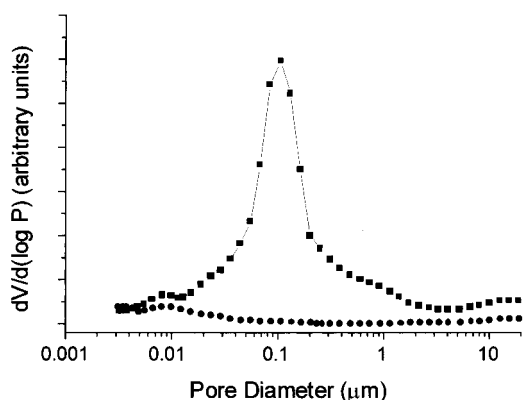


**Figure 2.** Mercury intrusion porosimetry data for polymer beads. Circle points: beads synthesized in the absence of  $\text{CO}_2$  (Table 1, entry 1); Square points: equivalent data for macroporous polymer beads synthesized using  $\text{scCO}_2$  as the porogen (300 bar, Table 1, entry 4); median pore diameter =  $110 \text{ nm}$ ; pore volume =  $1.23 \text{ cm}^3/\text{g}$ ; BET surface area =  $253 \text{ m}^2/\text{g}$ .

Macroporous polymer beads were formed when  $\text{CO}_2$  was added to the reaction mixture (Figures 1 and 2). Moreover, our preliminary results suggest that the degree of porosity, the average pore size, and the surface area in the beads can be tuned over a wide range by

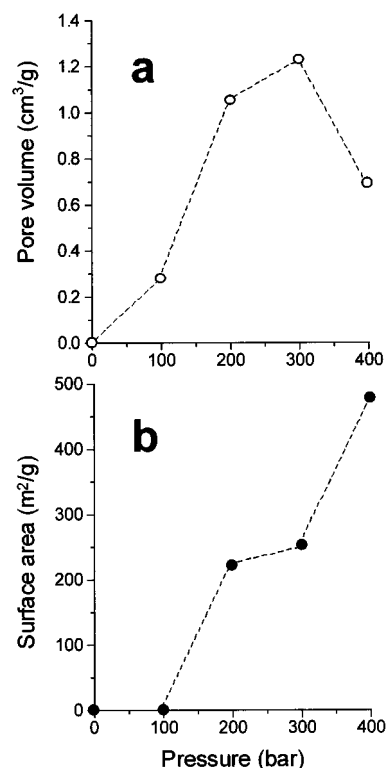


**Figure 3.** (a) Variation in pore volume of the macroporous beads as a function of reaction pressure, as measured by mercury intrusion porosimetry over the pore size range  $7 \text{ nm}$ – $20 \mu\text{m}$ . (b) Variation in BET surface area of the macroporous beads as a function of reaction pressure, as calculated from  $\text{N}_2$  adsorption/desorption isotherms.

varying the  $\text{CO}_2$  density. When the polymerization was carried out at 100 bar, porous beads were generated but the pore volume was relatively low ( $0.28 \text{ cm}^3/\text{g}$ ), as was the surface area of the sample ( $<5 \text{ m}^2/\text{g}$ ). This was explained by observation of the phase behavior, which showed that the monomer phase and the  $\text{CO}_2$  phase were not fully miscible at this temperature and pressure.<sup>16</sup> By contrast, at 200 bar, the monomer was completely miscible with  $\text{CO}_2$ , and a homogeneous monomer/ $\text{CO}_2$  mixture was dispersed as droplets throughout the aqueous phase. As a result, the beads were found to have increased pore volume ( $1.05 \text{ cm}^3/\text{g}$ ) and much higher surface area ( $222 \text{ m}^2/\text{g}$ ). When the synthesis was repeated at elevated  $\text{CO}_2$  pressures (300 and 400 bar), the products exhibited even greater surface areas, up to a maximum of  $478 \text{ m}^2/\text{g}$  at 400 bar (entry 5). This can be explained by the fact that the pore volume in the materials tended to increase with pressure (Figure 3a),<sup>17</sup> while the median pore diameter decreased significantly as the pressure was raised (Table 1). The combination of these two trends resulted in a sharp rise in polymer surface area as a function of  $\text{CO}_2$  pressure (Figure 3b). This variation in polymer structure is likely to stem from a combination of physical effects. At lower pressures ( $<100 \text{ bar}$ ), we observed that the monomer phase and the  $\text{CO}_2$  phase were not fully miscible. As the pressure was increased, more  $\text{CO}_2$  was dissolved in the monomer-rich droplets. This caused a change in the composition of the polymerization mixture and influenced polymer phase separation. The significant difference in morphology observed for the polymers synthesized at 100 and 200 bar may be attributed to this effect. However, at pressures in excess of 200 bar, we observed what appeared to be a single dispersed phase in the

reaction vessel (i.e., the monomer and CO<sub>2</sub> were fully miscible). Clearly, as the pressure was increased from 200 to 400 bar, yet more CO<sub>2</sub> was dissolved in the monomer droplets. However, in all of these experiments, the volumetric ratio of water to monomer was kept constant, while the CO<sub>2</sub> pressure was varied. Given that the surrounding water phase was relatively incompressible, then the combined *volume* of compressed CO<sub>2</sub> and monomer (i.e., the total volume of the dispersed phase) was approximately constant at the beginning of each experiment. This holds true even though the *molar* ratio of monomer to CO<sub>2</sub> varied dramatically.<sup>18</sup> As phase separation proceeds and the monomer is depleted, a CO<sub>2</sub> rich phase is formed which finally becomes the porous structure in the beads. As such, we believe that the variation in pore diameter (and the associated change in surface area) in the beads is affected by the *density* of the CO<sub>2</sub> phase, especially since systems of this type are known to be very sensitive to the porogen solvent quality.<sup>8–10,14</sup> The trends observed support this interpretation, with higher CO<sub>2</sub> densities (i.e., increased solvent strength) leading to smaller pores and larger surface areas. Broadly similar trends have been obtained for porous monolithic polymers synthesized in scCO<sub>2</sub>,<sup>5</sup> although direct comparison is difficult because one would expect differences in swelling behavior and polymer shrinkage phenomena due to interfacial effects which are present in the case of the suspension polymerizations.<sup>19</sup> Another factor to consider in these experiments is polymer plasticization. Previously, Quadir et al. studied the influence of scCO<sub>2</sub> on the kinetics of the surfactant-free O/W emulsion polymerization of methyl methacrylate (MMA).<sup>20</sup> In the case of linear polymers such as PMMA, the overall effect was a small change in molecular weight and molecular weight distribution. The authors ascribed this to plasticisation and swelling of the particles by scCO<sub>2</sub>, which reduces the viscosity and increases termination rates. Similar plasticization effects are also likely to have a significant impact on gelation kinetics<sup>21</sup> in suspension polymerizations carried out via our new route.

In addition to varying the CO<sub>2</sub> density, we are also investigating the influence of more standard reaction parameters such as monomer-to-cross-linker ratio, stirring speed, stabilizer morphology, and stabilizer concentration. The optimum stirring speed in this particular system appears to be around 600 rpm. Slower stirring leads to larger beads with much lower surface areas and intrusion volumes (entry 6), while faster stirring leads to a significant proportion of fractured beads and microparticulate “fines” (entry 7). As might be expected,<sup>9,11</sup> the level of cross-linking also has a strong effect on the properties of macroporous polymers prepared by this route (entry 8).

In conclusion, we have demonstrated that well-defined macroporous polymer beads can be synthesized in the absence of any organic solvents using scCO<sub>2</sub> as the porogen. These preliminary results are perhaps the most dramatic example yet of a system where polymer properties can be tuned by varying the supercritical fluid solvent density.

**Acknowledgment.** We gratefully acknowledge financial support from EPSRC (studentship award No. 99800424) and from Avecia Ltd (CASE Award to C.D.W.). We thank Dr. D. Pears and Dr. A. Shooter (Avecia Ltd) for assistance with BET measurements, and Dr. M. Cowan (Micromeritics Ltd) for Hg intrusion pore size

analysis. We also thank the Royal Society for provision of a Royal Society University Research Fellowship (to A.I.C.) and for a Royal Society Research Grant (No. 20372).

**Supporting Information Available:** Text giving synthetic procedures and characterization data (SEM, particle size distributions, BET) and figures showing electron micrographs and plots of particle size distributions, nitrogen adsorption and desorption analysis, and pressure–density relationships. This material is available free of charge via the Internet at <http://pubs.acs.org>.

## References and Notes

- Cooper, A. I. *J. Mater. Chem.* **2000**, *10*, 207–234.
- (a) Jessop, P. G.; Leitner, W. *Chemical Synthesis using Supercritical Fluids*; Wiley VCH: Weinheim, Germany, 1999. (b) Brennecke, J. F.; Chateaufneuf, J. E. *Chem. Rev.* **1999**, *99*, 433–452. (c) Oakes, R. S.; Clifford, A. A.; Bartle, K. D.; Petti, M. T.; Rayner, C. M. *Chem. Commun.* **1999**, *1999*, 247–248. (d) Clifford, A. A.; Pople, K.; Gaskill, W. J.; Bartle, K. D.; Rayner, C. M. *J. Chem. Soc., Faraday Trans.* **1998**, *94*, 1451–1456. (e) Beuermann, S.; Buback, M.; Schmaltz, C. *Macromolecules* **1998**, *31*, 8069–8074. (f) Canelas, D. A.; DeSimone, J. M. *Macromolecules* **1997**, *30*, 5673–5682. (g) Lepilleur, C.; Beckman, E. J. *Macromolecules* **1997**, *30*, 745–756.
- (a) Kendall, J. L.; Canelas, D. A.; Young, J. L.; DeSimone, J. M. *Chem. Rev.* **1999**, *99*, 543–563. (b) Mang, S. A.; Cooper, A. I.; Colclough, M. E.; Chauhan, N.; Holmes, A. B. *Macromolecules* **2000**, *33*, 303–308. (c) Christian, P.; Howdle, S. M.; Irvine, D. J. *Macromolecules* **2000**, *33*, 237–239. (d) Yates, M. Z.; Li, G.; Shim, J. J.; Maniar, S.; Johnston, K. P.; Lim, K. T.; Webber, S. *Macromolecules* **1999**, *32*, 1108–1026. (e) Canelas, D. A.; Betts, D. E.; DeSimone, J. M. *Macromolecules* **1996**, *29*, 9, 2818–2821. (f) DeSimone, J. M.; Maury, E. E.; Menciloglu, Y. Z.; McClain, J. B.; Romack, T. J.; Combes, J. R. *Science* **1994**, *265*, 356–359. (g) DeSimone, J. M.; Guan, Z.; Elsbernd, C. S. *Science* **1992**, *257*, 945–947.
- (a) Cooper, A. I.; Hems, W. P.; Holmes, A. B. *Macromol. Rapid Commun.* **1998**, *19*, 353–357. (b) Cooper, A. I.; Hems, W. P.; Holmes, A. B. *Macromolecules* **1999**, *32*, 2156–2166.
- (a) Cooper, A. I.; Holmes, A. B. *Adv. Mater.* **1999**, *11*, 1270–1274. (b) Cooper, A. I.; Wood, C. D.; Holmes, A. B. *Ind. Eng. Chem. Res.* **2000**, *39*, 4741–4744.
- Hodge, P.; Sherrington, D. C. *Syntheses and Separations using Functional Polymers*; Wiley: New York, 1989.
- Sherrington, D. C. *Chem. Commun.* **1998**, 2275–2286.
- (a) Yuan, H. G.; Kalfas, G.; Ray, W. H. *J. Macromol. Sci., Rev. Macromol. Chem. Phys.* **1991**, *C31*, 215–299. (b) Vivaldo-Lima, E.; Wood, P. E.; Hamielec, A. E.; Penlidis, A. *Ind. Eng. Chem. Res.* **1997**, *36*, 939–969.
- (a) Hamid, M. A.; Naheed, R.; Fuzail, M.; Rehman, E. *Eur. Polym. J.* **1999**, *35*, 1799–1811. (b) Lewandowski, K.; Svec, F.; Fréchet, J. M. J. *J. Appl. Polym. Sci.* **1998**, *67*, 597–607. (c) Horak, D.; Svec, F.; Ilavsky, M.; Bleha, M.; Baldrian, J.; Kalal, J. *Angew. Makromol. Chem.* **1981**, *95*, 117–127. (d) Horak, D.; Svec, F.; Bleha, M.; Kalal, J. *Angew. Makromol. Chem.* **1981**, *95*, 109–115.
- Liang, Y. C.; Svec, F.; Fréchet, J. M. J. *J. Polym. Sci., Part A: Polym. Chem.* **1997**, *35*, 2631–2643.
- (a) Schmid, A.; Flodin, P. *Makromol. Chem. Macromol. Chem. Phys.* **1992**, *193*, 1579–1589. (b) Howdle, S. M.; Jerabek, K.; Leocorbo, V.; Marr, P. C.; Sherrington, D. C. *Polymer* **2000**, *41*, 7273–7277.
- Nyhus, A. K.; Hagen, S.; Berge, A. *J. Appl. Polym. Sci.* **2000**, *76*, 152–169.
- Smigol, V.; Svec, F. *J. Appl. Polym. Sci.* **1993**, *48*, 2033–2039.
- (a) Peters, E. C.; Svec, F.; Fréchet, J. M. J. *Adv. Mater.* **1999**, *11*, 1169–1181. (b) Peters, E. C.; Petro, M.; Svec, F.; Fréchet, J. M. J. *Anal. Chem.* **1998**, *70*, 2288–2295. (c) Peters, E. C.; Svec, F.; Fréchet, J. M. J. *Chem. Mater.* **1997**, *9*, 1898–1902.
- See Supporting Information for full experimental details.
- This might also explain the rather polydisperse particle size distribution observed in this particular experiment.
- The cause of the apparent decrease in pore volume in the sample synthesised at 400 bar is as yet unknown but could

be a result of the fact that a significant proportion of the pores were too small to be detected by mercury intrusion porosimetry. The surface area of this sample is very high (478 m<sup>2</sup>/g) because of the low median pore diameter (40 nm).

- (18) Since the reactor has a fixed internal volume (57.5 cm<sup>3</sup>) and the volume of the aqueous phase was kept constant (46.0 cm<sup>3</sup>), then the combined volume of monomer and compressed CO<sub>2</sub> must also remain constant (11.5 cm<sup>3</sup>). However, the distribution of the compressed gas throughout the beads after phase separation clearly changes significantly as the CO<sub>2</sub> pressure is increased, as evident from the variation in pore size in samples 3–5. Thus, the molar ratio of monomer to porogen varies significantly from experiment to experiment while the volumetric ratio does not because the reactions are carried out in a sealed vessel of fixed volume. This is an unusual feature of polymerization reactions conducted using compressible supercritical fluid solvents.
- (19) (a) Otake, K.; Webber, S. E.; Munk, P.; Johnston, K. P. *Langmuir* **1997**, *13*, 3047–3051. (b) Svec, F.; Fréchet, J. M. J. *Chem. Mater.* **1995**, *7*, 707–715.
- (20) Quadir, M. A.; Snook, R.; Gilbert, R. G.; DeSimone, J. M. *Macromolecules* **1997**, *30*, 6015–6023.
- (21) Funke, W.; Okay, O.; Joos-Muller, B. *Adv. Polym. Sci.* **1998**, *136*, 139–234.

MA001514L